Renewable and Sustainable Energy Reviews 37 (2014) 778–793

Contents lists available at ScienceDirect

Renewable and Sustainable Energy Reviews

journal homepage: www.elsevier.com/locate/rser

A risk-based simulation and multi-objective optimization framework for the integration of distributed renewable generation and storage

Rodrigo Mena [a], Martin Hennebel [b], Yan-Fu Li [a], Carlos Ruiz [c], Enrico Zio [a,d,*]

[a] Chair on Systems Science and the Energetic Challenge, European Foundation for New Energy-Electricité de France, at École Centrale Paris—Supelec, Grande Voie des Vignes, F-92295 Châtenay-Malabry Cedex, France
[b] Supelec, Energy Department, F-91192 Gif-sur-Yvette Cedex, France
[c] Universidad Carlos III de Madrid, Department of Statistics, Avda. de la Universidad 30, 28911 Leganes, Madrid, Spain
[d] Politecnico di Milano, Energy Department, Via Ponzio 34/3, 20133 Milano, Milano, Italy

ARTICLE INFO

Article history:
Received 16 May 2013
Received in revised form
15 May 2014
Accepted 17 May 2014
Available online 10 June 2014

Keywords:
Distributed renewable generation
Uncertainty
Conditional value-at-risk
Simulation
Multi-objective optimization
Genetic algorithm

ABSTRACT

We present a simulation and multi-objective optimization framework for the integration of renewable generators and storage devices into an electrical distribution network. The framework searches for the optimal size and location of the distributed renewable generation units (DG). Uncertainties in renewable resources availability, components failure and repair events, loads and grid power supply are incorporated. A Monte Carlo simulation—optimal power flow (MCS-OPF) computational model is used to generate scenarios of the uncertain variables and evaluate the network electric performance. As a response to the need of monitoring and controlling the risk associated to the performance of the optimal DG-integrated network, we introduce the conditional value-at-risk (CVaR) measure into the framework. Multi-objective optimization (MOO) is done with respect to the minimization of the expectations of the global cost (C_g) and energy not supplied (ENS) combined with their respective CVaR values. The multi-objective optimization is performed by the fast non-dominated sorting genetic algorithm NSGA-II. For exemplification, the framework is applied to a distribution network derived from the IEEE 13 nodes test feeder. The results show that the MOO MCS-OPF framework is effective in finding an optimal DG-integrated network considering multiple sources of uncertainties. In addition, from the perspective of decision making, introducing the CVaR as a measure of risk enables the evaluation of trade-offs between optimal expected performances and risks.

Contents

1. Introduction . . . 779
2. Distributed generation network simulation model . . . 780
 2.1. Distributed generation network structure and configuration . . . 780
 2.2. Uncertainty modeling . . . 781
  2.2.1. Photovoltaic generation . . . 781
  2.2.2. Wind generation . . . 781
  2.2.3. Electric vehicles . . . 781
  2.2.4. Storage devices . . . 781
  2.2.5. Main power supply . . . 782
  2.2.6. Mechanical states of the components . . . 782
  2.2.7. Demand of power . . . 782
 2.3. Monte Carlo simulation . . . 782
 2.4. Optimal power flow . . . 783
 2.5. Performance indicators . . . 784
  2.5.1. Energy not supplied . . . 784

* Corresponding author. Tel.: +33 1 41131606.
E-mail addresses: rodrigo.mena@ecp.fr (R. Mena), martin.hennebel@supelec.fr (M. Hennebel), yanfu.li@ecp.fr (Y.-F. Li), caruizm@est-econ.uc3m.es (C. Ruiz), enrico.zio@ecp.fr, enrico.zio@polimi.it (E. Zio).

http://dx.doi.org/10.1016/j.rser.2014.05.046
1364-0321/

2.5.2. Global cost . . . 784
2.5.3. Risk . . . 784
3. DG units selection, sizing and allocation . . . 785
3.1. MOO problem formulation . . . 785
3.2. NSGA-II with nested MCS-OPF . . . 788
4. Case study . . . 788
4.1. Distribution network description . . . 788
4.2. Results and discussion . . . 789
5. Conclusions . . . 791
References . . . 792

1. Introduction

Over the last decade, the global energetic situation has been receiving a progressively greater attention. The adverse environmental effects of fossil fuels, the volatility of the energy market, the growing energy demand and the intensive reliance on centralized bulk-power generation have triggered a re/evolution towards cleaner, safer, diversified energy sources for reliable and sustainable electric power systems [1–6]. The challenges involved have stimulated both technological development of new equipment and devices, and efficiency improvements in design, planning, operation strategies and management across generation, transmission and distribution.

In this paper, we focus on distribution networks and the conceptual and operational transition they are facing. Indeed, the traditional passive operation with unidirectional flow supplied by a centralized generation/transmission system, is evolving towards an active operational setting with integration of distributed generation (DG) and possibly bidirectional power flows [7,8].

DG is defined as 'an electric power source connected directly to the distribution network or on the customer site of the meter' [8–10] and in principle offers important technical and economical benefits. Under the assumption that the distribution network operators have control over the dispatching of the DG power, improvement of the reliability of power supply and reduction of the power losses and voltages drops can be achieved. Indeed, DG allocation on areas close to the customers allows the power flowing through shorter paths, and therefore, decreasing the amount of unsatisfied power demand and enhancing the power and voltage profiles. Thus, the eventual intermittence of the centralized power supply can be smoothed [11]. In addition, the modular structure of the DG technologies implies lower financial risks [12,13] and thus the investments on the power system can be deferred [1,3].

Most of the actual DG technologies make use of local renewable energy resources, such as wind power, solar irradiation, hydropower, etc., which makes them even more attractive in view of the requested environmental sustainability (e.g., the Kyoto Protocol [7,14,15]). Given the intermittent character of these energy sources, their implementation needs to be accompanied by efficient energy storage technologies.

Attentive DG planning is needed to seize the potential advantages associated to DG integration, taking into account specific technical, operational and economic constraints, sources and loads forecasts and regulations. If the practice of selection, sizing and allocation of the different available technologies is not performed attentively, the installation of multiple renewable DG units could produce serious operational complications, in fact, counteracting the potential benefits. Degradation of control and protection devices, reduction of power quality and reliability on the supply, increment in the voltage instability and all related negative impacts on the costs, could become impediments for integration of DG [1–3,8,10,14,16–20].

Viewing DG planning as a fundamental baseline of advancement, many efforts have been made to solve the associated problem of DG allocation and sizing. Objective functions considered for the optimization are of economic, operational and technical type. Among the first type, cost-based objective functions have been used considering the costs of energy and fuel for generation, investments, operation and maintenance, energy purchase from the transmission system, energy losses, emissions, taxes, incentives, incomes, etc. [1–3,7,8,11,13,14,16–27]. The second type of operational objective functions mainly revolves around indexes such as the contingency load loss index (CLLI) [23], expected value of non-distributed energy cost (ECOST), system average interruption duration index (SAIDI), system average interruption frequency index (SAIFI) [7,16,28], expected energy not supplied (EENS) [28,29], among others. Regarding the third type of objective functions, technical performance indicators include energy losses [1,30] and total voltage deviation (TVD) [18].

Power Flow (PF) equations are typically solved within the optimization problem to evaluate the objective functions, while respecting constraints and incorporating non-convex and non-linear conditions. Given the complexity of the optimization problem, heuristic optimization techniques belonging to the class of Evolutionary Algorithms (EAs) have been proposed as a most effective way of solution [10], including particle swarm optimization (PSO) [23,24,27,31,32], differential evolution (DEA) [18] and genetic algorithms (GA) [3,7,11,13,14,16,26,33,34].

An additional difficulty associated to the problem is the proper modeling of the uncertainties inherent to the behavior of primary renewable energy sources and the unexpected operating events (failures or stoppages) that can affect the generation units. These uncertainties come on top of those already present in the network, such as intermittence and fluctuation in the main power supply due to unavailability of the transmission system, overloads and interruptions of the power flow in the feeders, failures in the control and protection devices, variability in the power loads and energy prices, etc. These uncertainties are incorporated into the modeling by generating a random set of scenarios by Monte Carlo simulation (MCS); the optimization is, then, executed to obtain the optimal expected or cumulative value(s) of the objective function (s) under the set of scenarios considered [2,3,7,16,28,32,34,35].

In the search for the optimal DG-integrated network, the use of only mean or cumulative values as objective function(s) of the optimization hinders the possibility of controlling the risk of the optimal solution(s): the optimal DG-integrated network may on average satisfy the performance objectives but be exposed to high-risk scenarios with non-negligible probabilities [1,7,16,24,28,36].

The original contributions of this work reside in: addressing the optimal renewable DG technology selection, sizing and allocation problem within a simulation and multi-objective optimization (MOO) framework that allows for assessing and controlling risk; introducing the conditional value-at-risk (CVaR) as a measure of the risk associated to each objective function of the optimization

[37,38]. The main sources of uncertainty are taken into account through the implementation of a MCS and OPF (MCS-OPF) resolution engine nested in a MOO based on NSGA-II [39]. The aim of the MOO is, specifically, the simultaneous minimization of the expected global cost (EC_g) and expected energy not supplied (*EENS*), and corresponding *CVaR* values. A weighting factor β is introduced to leverage the impact of the *CVaR* in the search of the final Pareto optimal renewable DG integration solutions. The proposed framework provides a new spectrum of information for well-supported decision making, enabling the trade-off between optimal expected performance and the associated risk to achieve it.

2. Distributed generation network simulation model

This section introduces the MCS-OPF model, including the definition of the DG structure and configuration, the presentation of the uncertainty sources and their treatment, the MCS for scenarios generation and the OPF formulation for evaluating the performance of the distribution network, in terms of the objective functions of the MOO problem. The outputs of the MCS-OPF model are the probability density functions of the energy not supplied (*ENS*) and the global cost (C_g) of the network, and their respective *CVaR* values.

2.1. Distributed generation network structure and configuration

Four main classes of components are considered in the distribution network: nodes, feeders, renewable DG units and main power supply spots (MS). The nodes can be understood as fixed spatial locations at which generation units and loads can be allocated. Feeders connect different nodes and through them the power is distributed. Renewable DG units and main power supply spots are power sources; in the case of electric vehicles and storage devices they can also act as loads when they are in charging state. The locations of the main supply spots are fixed. The MOO aims at optimally allocating renewable DG units at the different nodes. Fig. 1 shows an example of configuration of a distribution network adapted from the *IEEE* 13 *nodes test feeder* [40], for which the regulator, capacitor, switch and the feeders with length equals to zero are neglected.

Each component in the distribution network has its own features and operating states that determine its performance. Assuming stationary conditions of the operating variables, the network operation is characterized by the location and magnitude of power available, the loads and the mechanical states of the components, because degradation or failures can have a direct impact on the power availability (in the DG units, feeders and/or main supply).

The renewable DG technologies considered in this work include solar photovoltaic (PV), wind turbines (W), electric vehicles (EV) and storage devices (batteries) (ST). The power output of each of these technologies is inherently uncertain. PV and W generation are subject to variability through their dependence on environmental conditions, i.e., solar irradiance and wind speed. Dis/connection and dis/charging patterns in EV and ST, respectively, further influence the uncertainty in the power outputs from the DG units. Also generation and distribution interruptions caused by failures are regarded as significant.

The following notation is used for sets and subsets of components in the distribution network:*N*—set of all nodes; *MS*—set of all types of main supply power sources; *DG*—set of all DG technologies; *PV*—set of all photovoltaic technologies; *W*—set of all wind technologies; *EV*—set of all electric vehicle technologies; *ST*—set of all storage technologies; *FD*—set of all feeders.

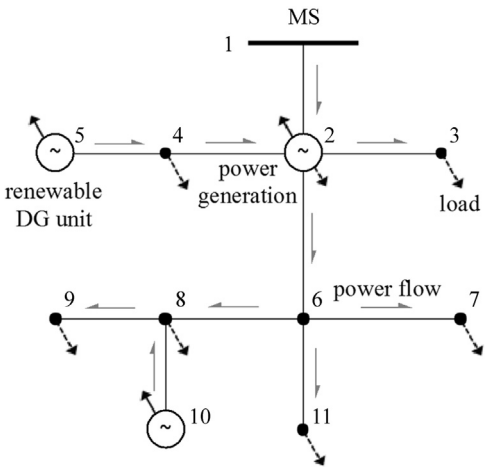

Fig. 1. Example of distribution network configuration.

The configurations of power sources allocated in the network, indicating the size of power capacity and the location, is given in matrix form:

$$\Xi = \begin{array}{c} \begin{matrix} \mathrm{MS}_1 & \cdots & \mathrm{MS}_j & \cdots & \mathrm{MS}_m & \mathrm{DG}_1 & \cdots & \mathrm{DG}_j & \cdots & \mathrm{DG}_d \end{matrix} \\ \left[\begin{array}{ccccc|ccccc} \xi_{1,1} & \cdots & \xi_{1,j} & \cdots & \xi_{1,m} & \xi_{1,m+1} & \cdots & \xi_{1,m+j} & \cdots & \xi_{1,m+d} \\ \vdots & \ddots & \vdots & \ddots & \vdots & \vdots & \ddots & \vdots & \ddots & \vdots \\ \xi_{i,1} & \cdots & \xi_{i,j} & \cdots & \xi_{i,m} & \xi_{i,m+1} & \cdots & \xi_{i,m+j} & \cdots & \xi_{i,m+d} \\ \vdots & \ddots & \vdots & \ddots & \vdots & \vdots & \ddots & \vdots & \ddots & \vdots \\ \xi_{n,1} & \cdots & \xi_{n,j} & \cdots & \xi_{n,m} & \xi_{n,m+1} & \cdots & \xi_{n,m+j} & \cdots & \xi_{n,m+d} \end{array}\right] \text{ node } i \\ \underbrace{\qquad\qquad\qquad\qquad\qquad}_{\Xi^{MS}} \qquad \underbrace{\qquad\qquad\qquad\qquad\qquad\qquad\qquad\qquad\qquad}_{\Xi^{DG}} \\ \begin{array}{cc} \text{fixed size and} & \text{decision matrix of type, size} \\ \text{location of MS} & \text{and location of DG units} \end{array} \end{array} \tag{1}$$

where Ξ—*configuration matrix* of type, size and location of the power sources allocated in the distribution network; Ξ^{MS}—size and location of main supply, fixed part of the configuration matrix; Ξ^{DG}—type size and location of DG units, decision variable part of the configuration matrix; *n*—number of nodes in the network, |*N*|; *m*—number of main supply type (transformers), |*MS*|; *d*—number of DG technologies, |*DG*|.

$$\xi_{i,j} = \begin{cases} \zeta & \text{number of units of the MS type or DG technology } j \text{ allocated at node } i \\ 0 & \text{otherwise} \end{cases}$$
$$\forall i \in N, j \in MS \cup DG, \zeta \in Z^* \tag{2}$$

Feeders deployment is described by the set of pairs of nodes connected:

$$FD = \{(1,2), \ldots, (i,i')\} \quad \forall (i,i') \in N \times N, (i,i') \text{ is a feeder} \tag{3}$$

Any configuration $\{\Xi, FD\}$ of power sources $\Xi = [\Xi^{MS} | \Xi^{DG}]$ and feeders *FD* of the distribution network are affected by uncertainty, so that the operation and performance of the distribution network is strongly dependent on the network configuration and scenarios. Furthermore, if the distribution network acts as a 'price taker', the variability of the economic conditions, particularly the price of the energy, is also an influencing factor [13,19,20]. For these reasons, it is imperative to represent and account for the uncertainties in the optimal allocation results for informed and conscious decision-making.

2.2. Uncertainty modeling

2.2.1. Photovoltaic generation

PV technology converts the solar irradiance into electrical power through a set of solar cells configured as panels. Commonly, solar irradiance has been modeled using probabilistic distributions, derived from the weather historical data of a particular geographical area. The Beta distribution function [41,42] is used in this paper:

$$f_{pv}(s)=\begin{cases}\frac{\Gamma(\alpha+\beta)}{\Gamma(\alpha)\Gamma(\beta)}s^{(\alpha-1)}(1-s)^{(\beta-1)} & \forall s\in[0,1],\alpha\geq 0,\beta\geq 0\\ 0 & \text{otherwise}\end{cases} \quad (4)$$

where s—solar irradiance; f_{pv}—beta probability density function; α, β—parameters of the beta probability density function.

The parameters of the Beta probability density function can be inferred from the estimated mean μ and standard deviation σ of the random variable s as follows [1]:

$$\beta=(1-\mu)\left(\frac{\mu(1+\mu)}{\sigma^2}-1\right) \quad (5)$$

$$\alpha=\frac{\mu\beta}{1-\mu} \quad (6)$$

Besides dependence on solar irradiation, PV depends also on the features of the solar cells that constitute the panels and on ambient temperature on site. The power outputs from a single solar cell is obtained from the following equations [41,42]:

$$T_c=T_a+s\left(\frac{N_{oT}-20}{0.8}\right) \quad (7)$$

$$I=s(I_{sc}+k_i(T_c-25)) \quad (8)$$

$$V=V_{oc}+k_vT_c \quad (9)$$

$$FF=\frac{V_{MPP}I_{MPP}}{V_{oc}I_{sc}} \quad (10)$$

$$P^{pv}(s)=n_{\text{cells}}FF\times V\times I \quad (11)$$

where T_a—ambient temperature [°C]; N_{oT}—nominal cell operating temperature [°C]; T_c—cell temperature [°C]; I_{sc}—short circuit current [A]; k_i—current temperature coefficient [mA/°C]; V_{oc}—open circuit voltage [V]; k_v—voltage temperature coefficient [mV/°C]; V_{MPP}—voltage at maximum power [V]; I_{MPP}—current at maximum power [A]; FF—fill factor; n_{cells}—number of photovoltaic cells; $P^{pv}(s)$—PV power output [W].

2.2.2. Wind generation

Wind generation is obtained from turbine-alternator devices that transform the kinetic energy of the wind into electrical power. The stochastic behavior of the wind speed is commonly represented through probability distribution functions. In particular, the Rayleigh distribution has been found suitable to model the randomness of the wind speed in various conditions [1,42]:

$$f_w(ws)=\frac{2ws}{\sigma}e^{-(ws/\sigma)^2} \quad (12)$$

where ws—wind speed [m/s]; f_w—Rayleigh probability density function; σ—scale parameter of the Rayleigh distribution function.

Then, for a given wind speed value, the power output of one wind turbine can be determined as [1,41,42]:

$$P^w(ws)=\begin{cases}P^w_{RTD}\frac{ws-ws_{ci}}{ws_a-ws_{ci}} & \text{if } ws_{ci}\leq ws<ws_a\\ P^w_{RTD} & \text{if } ws_a\leq ws<ws_{co}\\ 0 & \text{otherwise}\end{cases} \quad (13)$$

where ws_{ci}—cut-in wind speed [m/s]; ws_a—rated wind speed [m/s]; ws_{co}—cut-out wind speed [m/s];P^w_{RTD}—rated power [kW]; $P^w(ws)$—wind power output [kW].

2.2.3. Electric vehicles

In this work, EV are considered as battery electric vehicles with three possible operating states: charging, discharging (i.e., injecting power into the distribution network) and disconnected [43]. To model their pattern of operation, they are considered as a 'block group', aggregating their single operating states into an overall performance. The main reasons for this aggregation are the observed nearly stable daily usage schedule of EV and the need of avoiding the combinatorial explosion of the model [42].

The power output of one block of EV is formulated by assigning residence time intervals to each possible operating state and associating them with the percentage of trips that the vehicles perform by hour of a day [43]. This allows approximating the hourly probability distribution of the operating states per day, as shown Fig. 2. In a given (random) scenario of operational conditions, the determination of the operating state of a block of EV, of a specific hour of the day, is sampled randomly from the corresponding probability distribution. Accordingly, the power output for a unit or block group of EV is calculated using the expressions below:

$$f_{ev}(t_d,op)=\begin{cases}p_{dch}(t_d) & \text{if } op=\text{discharging}\\ p_{ch}(t_d) & \text{if } op=\text{charging}\\ p_{dtd}(t_d) & \text{if } op=\text{disconnected}\end{cases} \quad \forall op\in OPs=\{\text{charging, discharging, disconnected}\} \quad (14)$$

$$P^{ev}(op)=\begin{cases}P^{ev}_{RTD} & \text{if } op=\text{discharging}\\ -P^{ev}_{RTD} & \text{if } op=\text{charging}\\ 0 & \text{if } op=\text{disconnected}\end{cases} \quad \forall t\in[0,t_{Rop}],op\in OPs=\{\text{charging, discharging, disconnected}\} \quad (15)$$

where t_d—hour of the day [h]; t_{Rop}—residence time interval for operating state op [h]; f_{ev}—operating state probability density function; P^{ev}_{RTD}—rated power [kW].

2.2.4. Storage devices

Analogously to the EV case, storage devices are treated as batteries. In reality, these present two main operating states, charging and discharging [44]. However, for this study the level of charge in the batteries is randomized and the state of discharging is the only one that is allowed. This is done to simplify the behavior of the batteries, making it independent on the previous state of charge. The discharging time interval is assigned according to the relation between the batteries rated power, their energy density and the random level of charge they present. For this, the discharging action is carried out at a rate equal to the rated power. Then, the power output per unit of mass of active chemical in the

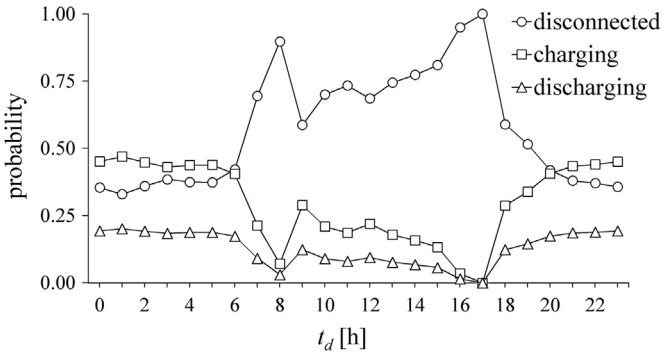

Fig. 2. Hourly probability distribution of EV operating states per day.

battery M_T is estimated as follows:

$$f_{st}(Q^{st}) = \begin{cases} \frac{1}{SE \times M_T} & \forall Q^{st} \in [0, SE \times M_T] \\ 0 & \text{otherwise} \end{cases} \quad (16)$$

$$t'_R(Q^{st}) = \frac{Q^{st}}{P^{st}_{RTD}} \quad (17)$$

$$P^{st}(t_R) = P^{st}_{RTD} \quad \forall t_R \in [0, t'_R] \quad (18)$$

where Q^{st}—level of charge in the battery [kJ]; SE—specific energy of the active chemical [kJ/kg]; M_T—total mass of the active chemical in the battery [kg]; f_{st}—uniform probability density function; ${P_{RTD}}^{st}$—rated power [kW]; t'_R—discharging time interval [h].

2.2.5. Main power supply

The MS spots in the distribution network are the power stations connected to the transmission system. The distribution transformers are located on these spots and provide the voltage level of the customers. The stochasticity of the available main supplies of power is represented following normal distributions [10,45], truncated by the maximum capacity of the transformers.

$$f_{pv}(s) = \begin{cases} \frac{\frac{1}{\sigma^{ms}}\phi((P^{ms} - \mu^{ms})/\sigma^{ms})}{\Phi((P^{ms}_{cap} - \mu^{ms})/\sigma^{ms}) - \Phi(-\mu^{ms}/\sigma^{ms})} & \forall P^{ms} \in [0, P^{ms}_{cap}] \\ 0 & \text{otherwise} \end{cases} \quad (19)$$

where P^{ms}—available main power supply [kW]; μ^{ms}—Normal distribution mean; σ^{ms}—Normal distribution standard deviation; f_{ms}—Normal probability density function; P^{ms}_{ccp}—maximum capacity of the transformer [kW]; ϕ—standard Normal probability density function; Φ—cumulative distribution function of ϕ.

2.2.6. Mechanical states of the components

Renewable DG units, MS spots and feeders are subject to wearing and degradation processes. These processes can trigger unexpected events, even failures, interrupting or reducing the specific functionality of each component. Frequently, the stochastic behavior of failures, repairs and maintenance actions is modeled using Markov models [28,42]. In this work, a two-state model is implemented in which the components can be in the mutually exclusive states: *available to operate* and *under repair* (failure state). Assuming the duration of each state as exponentially distributed, the mechanical state of a component can be randomly generated as follows:

$$mc = \begin{cases} 1 & \text{if the component is available to operate} \\ 0 & \text{otherwise} \end{cases} \quad \forall \text{component} \in \{\Xi, FD\} \quad (20)$$

$$f_{mc}(mc) = \frac{(1-mc)\lambda^F + mc\lambda^R}{\lambda^F + \lambda^R} \quad \forall mc \in \{0, 1\} \quad (21)$$

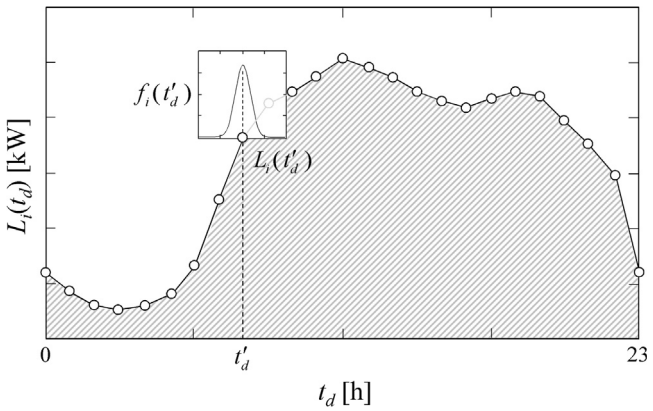

Fig. 3. Daily load profile. Hourly normally distributed load.

where mc—binary mechanical state variable, λ^F—failure rate [failures/h], λ^R—repair rate [repairs/h,], f_{mc}—mechanical state probability mass function.

2.2.7. Demand of power

Overall demands of power, as well as single load profiles in the nodes of the distribution network, can be obtained as daily load curves in which to each hour corresponds one specific level of load, inferred from historical data [1,14,19]. In addition, power demands profiles can be considered uncertain following normal distributions [34].

Within the proposed modeling framework, the nodal demands of power are defined by integrating the two models mentioned above, i.e., adopting the general daily load profile and considering the hourly levels of load as normally distributed. Fig. 3 schematizes the previous assumption for a generic node i.

In this manner, the nodal demand of power is deducted from the overall demand in the network, and modeled as:

$$f_{L_i}(L_i, t_d) = \begin{cases} \frac{\frac{1}{\sigma_i(t_d)}\phi((L_i - \mu_i(t_d))/\sigma_i(t_d))}{1 - \Phi(-\mu_i(t_d)/\sigma_i(t_d))} & \forall i \in N, L_i \in [0, \infty] \\ 0 & \text{otherwise} \end{cases} \quad (22)$$

where t_d—hour of the day [h], L_i—power demand in node i [kW], μ_i—normal distribution mean of power demand in node i, σ_i—normal distribution standard deviation of power demand in node i, f_{Li}—normal probability density function of power demand in node i.

2.3. Monte Carlo simulation

Most of the techniques used for evaluating the performance of renewable DG-integrated distribution networks are of two classes: analytical methods and MCS [28]. The implementation of analytical methods is always preferable, in theory, because of the possibility of achieving closed exact solutions, but in practice; it often requires strongly simplifying assumptions that may lead to unrealistic results: power network applications exist but for non-fluctuating or non-intermittent generation and/or load profiles, and low dimensionality of the network, gaining traceability with reduced computational efforts [32]. Different, MCS techniques allow considering more realistic models that analytical methods do, because simplifying assumptions are not necessary to solve the model, since *de facto* the model is not solved but simulated and the quantities of interest are estimated from the statistics of the virtual simulation runs [46]. For this reason MCS is quite adequate for application on the analysis of distribution networks with significant randomness or variability in the sources of power supply and loads, failure occurrence and strong dependence on the power flows as a consequence of congestion conditions in the feeders, etc.

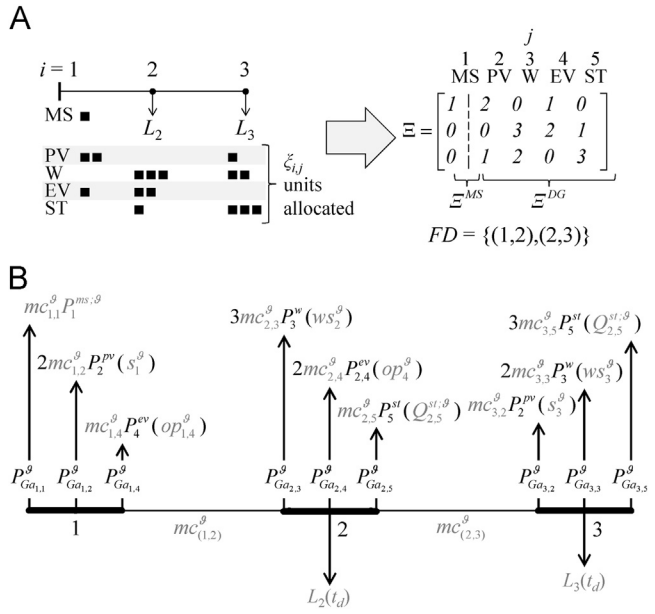

Fig. 4. Example of the matrix form construction of a DG-integrated network (A) and schema of the operating state definition from the sampled variables (B).

[3,31,33,41,42,47]; the price to pay for this is the possibly considerable increment in the use of computational resources, and various methods exist to tackle this problem [46].

Given the multiple sources of uncertainties considered in the proposed framework and the proven advantages of MCS for adequacy assessment of power distribution networks with uncertainties [3,31,33,41,42,47], we adopt a non-sequential MCS to emulate the operation of a distribution network, sampling the uncertain variables without considering their time dependence, so as to reduce the computational problem.

For a given structure and configuration of the distribution network $\{\Xi,FD\}$, i.e., for the fixed Ξ^{MS} and FD deployments and the proposed renewable DG integration plan denoted by Ξ^{DG}, each uncertain variable is randomly sampled. The set ϑ of sampled variables constitutes an operational scenario, in correspondence of which the distribution network operation is modeled by OPF and its performance evaluated. The two inputs to the OPF model are the network configuration $\{\Xi,FD\}$ and the operational conditions scenario ϑ.

$$\vartheta = [t_d, P^{ms}_{i,j}, L_i, s_i, ws_i, Q^{st}_{i,j}, mc_{i,j}, mc_{(i,i')}] \quad \forall i,i' \in N, j \in MS \cup DG, (i,i') \in FD \tag{23}$$

where t_d—hour of the day [h], randomly sampled from a discrete uniform distribution $U(1,24)$.

Fig. 4 shows an example of the matrix form construction of the DG-integrated distribution network, considering a simple case of $n=3$ nodes. The network contains one MS spot at node $i=1$, defining the fixed part Ξ^{MS} of the configuration matrix, whereas, the decision variable Ξ^{DG} proposes a renewable DG integration plan Ξ^{DG} that built from the number of units ξ of each DG technology allocated. In this way, the network configuration $\{\Xi,FD\}$ is composed by the matrix $\Xi=[\Xi^{MS} \mid \Xi^{DG}]$ and the deployment of feeders. Then, given the spatial representation $\{\Xi, FD\}$, the sampling of the scenario ϑ determines the operational conditions to perform power flow analysis, i.e., distribute the power available P^{ϑ}_{Ga} to supply appropriately the demands L_i.

The available power in the power source type j at node i, $P^{\vartheta}_{Ga_{i,j}}$, is function of the number of units allocated $\xi_{i,j}$, the mechanical state $mc_{i,j}$ and the specific unitary power output function $G_j$associated to the generation unit j, formulated in Eqs. (24) and (25).

$$P^{\vartheta}_{Ga_{i,j}} = \xi_{i,j} mc^{\vartheta}_{i,j} G_j(\vartheta) \tag{24}$$

$$G_j(\vartheta) = \begin{cases} P^{ms;\vartheta}_j & \text{if } j \in MS \\ P^{pv}_j(s^{\vartheta}_i) & \text{if } j \in PV \\ P^{w}_j(ws^{\vartheta}_i) & \text{if } j \in W \\ P^{ev}_j(op^{\vartheta}_{i,j}) & \text{if } j \in EV \\ P^{st}_j(Q^{st;\vartheta}_{i,j}) & \text{if } j \in ST \end{cases} \quad \forall i \in N \tag{25}$$

In the proposed non-sequential MCS procedure, the intermittency in the solar irradiation is taken into account defining a night interval between 22.00 and 06.00 h, i.e., if the value of the hour of the day t_d (h), sampled from a discrete uniform distribution U (1,24), falls in the night interval, there is no solar irradiation. Regarding the wind speed, its variability is considered by sampling positive values from a Rayleigh probability density function fitted on historical data and whose parameters as such that the probability of absence of wind is zero. Since it is not reasonable to force the historical profile of the wind speed to follow a distribution that admits intermittency, a common alternative technique is to model the wind by a Markov Chain. Indeed, it is possible to accurately represent the wind speed by a stationary Markov process if the historical profile of wind speed data is sufficiently large e.g., years [28]. The intermittency is, then, represented by the first state of the chain with wind speed equals to zero, and the sampling of the wind speed states in the non-sequential MCS of the proposed framework, can be performed using the steady-state probabilities of the Markov Chain.

An important issue in modeling the operation of power systems is how to represent the evolution of uncertain operating conditions, such as solar irradiation, wind speed, load profiles, energy prices, among others. As an example, the load forecast implies the prediction of future power demands given specific previous conditions. Therefore, to consider load forecast uncertainty within the proposed MCS framework, it would be necessary to change to a sequential simulation model, in which the uncertain renewable energy resources, main power supply and loads must be sampled at each time step. In particular, load forecast uncertainty can be integrated properly building consecutive load scenarios and assigning corresponding probabilities of occurrence as presented by [7,48]. Another interesting approach for load forecast uncertainty modelling is the geometric Brownian motion (GBM) stochastic process [31,49].

2.4. Optimal power flow

Power flow analysis is performed by DC OPF [50] which takes into account the active power flows, neglecting power losses, and assumes a constant value of the voltage throughout the network. This allows transforming to linear the classic non-linear power flow formulation, gaining simplicity and computational tractability. For this reason, DC power flow is often used in techno-economic analysis of power systems, more frequently in transmission [50,51] but also in distribution networks [51].

The DC power flow generic formulation is:

$$P_i = \sum_{i' \in N} B_{i,i'}(\delta_i - \delta_{i'}) \quad \forall i,i' \in N, (i,i') \in FD \tag{26}$$

$$\sum_{i \in N} (P_{Gi} - L_i - P_i) = 0 \quad \forall i \in N \tag{27}$$

where, P_i—active power leaving node i [kW]; $B_{i,i'}$ susceptance of the feeder (i,i') [1/Ω]; δ_i—voltage angle at node i; P_{Gi}—active power

injected or generated at node i [kW]; L_i—load at node i [kW].The assumptions are:

- the difference between voltage angles are small, i.e., $sin(\Delta\delta) \approx \delta$, $cos(\Delta\delta) \approx 1$
- the feeders resistance are neglected, i.e., $R \ll X$, which implies that power losses in the feeder are also neglected
- the voltage profile is flat (constant V, set to 1 p.u.)

Then, for a given configuration $\{\Xi, FD\}$ and operational scenario ϑ the formulation of the OPF problem is:

$$\min \quad C_{O\&M}^{net;\vartheta}(P_{Gu}^{\vartheta}) = \sum_{i \in Nj \in MS \cup DG} \sum C_{O\&M_j^v} P_{Gu_{i,j}}^{\vartheta} t^S \tag{28}$$

s.t.

$$L_i^{\vartheta} - \sum_{j \in MS \cup DG} P_{Gu_{i,j}}^{\vartheta} - \sum_{i' \in N} mc_{(i,i')}^{\vartheta} B_{(i,i')}(\delta_i^{\vartheta} - \delta_{i'}^{\vartheta}) - LS_i^{\vartheta} = 0 \quad \forall i, i' \in N, (i,i') \in FD \tag{29}$$

$$P_{Gu_{i,j}}^{\vartheta} \le P_{Ga_{i,j}}^{\vartheta} \quad \forall i \in N, j \in MS \cup DG \tag{30}$$

$$0 \le P_{Gu_{i,j}}^{\vartheta} \quad \forall i \in N, j \in MS \cup DG \tag{31}$$

$$mc_{(i,i')}^{\vartheta} B_{(i,i')}(\delta_i^{\vartheta} - \delta_{i'}^{\vartheta}) \le V \times Amp_{(i,i')} \quad \forall i, i \in N, (i,i') \in FD \tag{32}$$

$$-mc_{(i,i')}^{\vartheta} B_{(i,i')}(\delta_i^{\vartheta} - \delta_{i'}^{\vartheta}) \le V \times Amp_{(i,i')} \quad \forall i, i' \in N, (i,i') \in FD \tag{33}$$

where, t^S—duration of the scenario [h]; $C_{O\&M}^{net;\vartheta}$—operating and maintenance costs of the total power supply and generation [$];$C_{O\&M_j^v}$—operating and maintenance variable costs of the power source j [$/kW h]; $mc_{(i,i')}^{\vartheta}$—mechanical state of the feeder (i,i'); $B_{i,i'}$—susceptance of the feeder (i,i'), [1/Ω]; $mc_{i,j}^{\vartheta}$, mechanical state of the power source j at node i; $P_{Ga_{i,j}}^{\vartheta}$—available power in the source j at node i [kW]; $P_{Gu_{i,j}}^{\vartheta}$; power produced by source j at node i [kW]; LS_i^{ϑ}—load shedding at node i [kW]; V—nominal voltage of the network [kV]; $Amp_{(i,i')}$—ampacity of the feeder (i,i'), [A].

The load shedding in the node i, LS_i, is defined as the amount of load(s) disconnected in node i to alleviate overloaded feeders and/or balance the demand of power with the available power supply [52].

The OPF objective is the minimization of the operating and maintenance costs associated to the generation of power for a given scenario ϑ of duration t^S. Eq. (29) corresponds to the power balance equation at node i, while Eqs. (30) and (31) are the bounds of the power generation and Eqs. (32) and (33) account for the technical limits of the feeders.

2.5. Performance indicators

Given a set Υ of ns sampled operational scenarios ϑ_ℓ, $\ell \in \{1,\ldots,ns\}$, the OPF is solved for each scenario $\vartheta_\ell \in \Upsilon$, giving in output the values of ENS and global cost.

2.5.1. Energy not supplied

ENS is a common index for reliability evaluation in power systems [1,10,11,48,49,52–55]. In the present work, its value is obtained directly from the OPF output in the form of the aggregation of all-nodal load sheddings per scenario ϑ_ℓ:

$$ENS^{\vartheta_\ell} = \sum_{i \in N} LS_i^{\vartheta_\ell} \times t^S \quad \forall \vartheta_\ell \in \Upsilon \tag{34}$$

$$ENS^{\Upsilon} = \{ENS^{\vartheta_1}, \ldots, ENS^{\vartheta_\ell}, \ldots, ENS^{\vartheta_{ns}}\} \tag{35}$$

2.5.2. Global cost

The C_g of the distribution network is formed by two terms, fixed and variable costs. The former term includes those costs paid at the beginning of the operation after the installation of the DG (conception of Ξ^{DG}). They are the investment-installation cost and the operation-maintenance fixed cost. The variable term refers to the operating and maintenance costs. Note that these costs are dependent on the power generation and supply, which are a direct output of the OPF (Eq. (28)). In addition, this term considers revenues associated to the renewable sources incentives. Considering the distribution network as a 'price taker' entity, the profits depend on the value of the energy price that is correlated with the total load in the network. Three different ranges of load are considered for the daily profile. For each range, a correlation value of energy price is considered as shown in Fig. 5(A).

In Fig. 5(B) the correlation between energy price and total load is presented as the proportion of their maximum values. As an intermediate approximation of existing studies (e.g., [13,19,20]), the line with square-markers represents the proportional correlation used in this study, which can be expressed as:

$$ep = ep_h\left(-0.38\left(\frac{L_T(t_d)}{L_{Th}}\right)^2 + 1.38\frac{L_T(t_d)}{L_{Th}}\right) \tag{36}$$

Thereby, the global cost function for a scenario ϑ_ℓ is given by:

$$C_g^{\vartheta_\ell} = \sum_{i \in Nj \in DG} \sum (C_{inv_j} + C_{O\&M_j^f})\left(\frac{t^S}{t^h}\right) + C_{O\&M}^{net;\vartheta_\ell} - (inc + ep(L_T^{\vartheta_\ell})) \sum_{i \in Nj \in DG} \sum P_{Gu_{i,j}}^{\vartheta_\ell} t^S \forall \vartheta_\ell \in \Upsilon \tag{37}$$

$$C_g^{\Upsilon} = \{C_g^{\vartheta_1}, \ldots, C_g^{\vartheta_\ell}, \ldots, C_g^{\vartheta_{ns}}\} \tag{38}$$

where C_{inv_j}—investment cost of the DG technology j [$]; $C_{O\&M_j^f}$—operating and maintenance fixed costs of the DG technology j [$]; t^h—horizon of analysis [h]; inc—incentive for generation from renewable sources [$/kW h]; ep—energy price [$/kW h]; $C_g^{\vartheta_\ell}$—global cost [$].

2.5.3. Risk

In [38], the importance of measuring risk when optimizing under uncertainty and including it as part of the objective function (s) or constraints is emphasized. The proposed MOO framework introduces the $CVaR$ as a coherent measure of the risk associated to the objective functions of interest. The $CVaR$ has been broadly used in financial portfolio optimization either to reduce or minimize the probability of incurring in large losses [37,38]. This risk measurement allows evaluating how 'risky' is the selection of a solution leading to a determined value of expected losses.

We can consider a fixed configuration of the distribution network $\{\Xi, FD\}$ including the integration of DG units as a 'portfolio'. The assessed expectations of ENS^{Υ} and C_g^{Υ}, found from the MCS-OPF applied to the set of scenarios Υ, are estimations of the 'losses'; then, $CVaR(ENS^{\Upsilon})$ and $CVaR(C_g^{\Upsilon})$ represent the risk associated to the solutions with these expectations.

The definition of $CVaR$ for continuous and discrete general loss functions is given in detail in [38]. Here a simplified and intuitive manner to understand the $CVaR$ definition and its derivation according to [56] is presented.

As shown in Fig. 6(A), for a discrete approximation of the probability of the losses, given a confidence level or α-percentile, the value-at-risk VaR_α represents the smallest value of $losses$ for which the probability that the losses do not exceed the value of VaR_α is greater than or equal to α. Thus, from the cumulative distribution function $F(losses)$ is possible to construct the α-tail cumulative distribution function $F_\alpha(losses)$ for the losses, such that

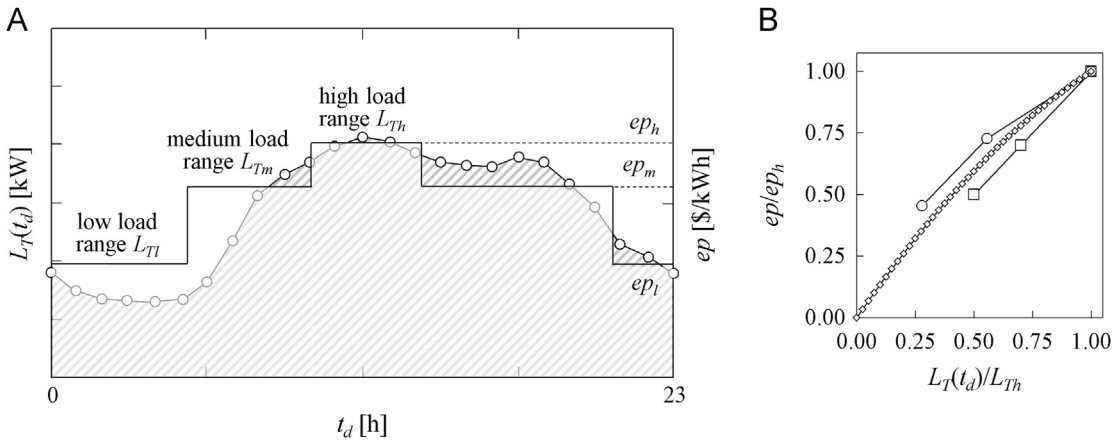

Fig. 5. Example of load ranges definition for a generic daily load profile (A) and correlation energy price-total load (B) [13,19,20].

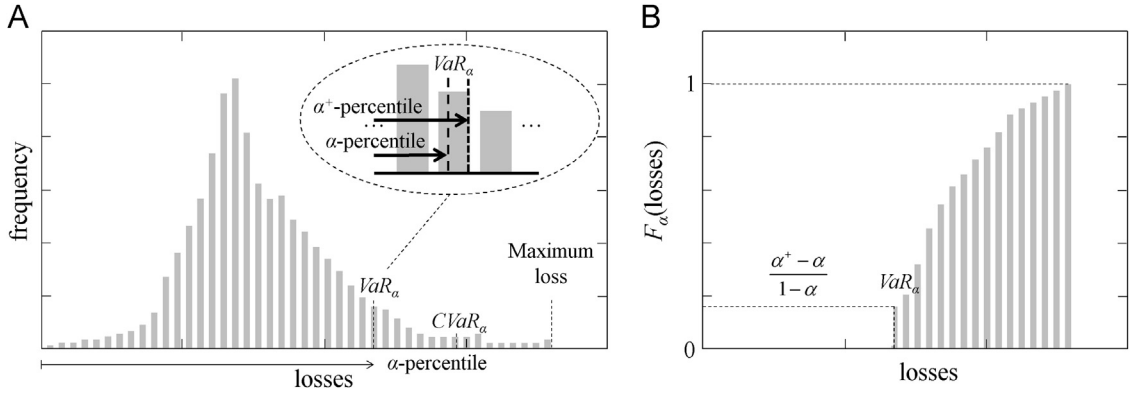

Fig. 6. Graphic representation of the *CVaR*.

(Fig. 6(B)):

$$F_\alpha(losses) = \begin{cases} \frac{F(losses)-\alpha}{1-\alpha} & \text{if } VaR_\alpha \le losses \\ 0 & \text{otherwise} \end{cases} \tag{39}$$

The α-tail cumulative distribution function represents the risk 'beyond the *VaR*' and its mean value corresponds to the $CVaR_\alpha$.

Among other risk measures, the *CVaR* has been commonly used to assess the financial impact associated to different sources of uncertainty on electricity markets behavior. Some interesting approaches in the use of diverse risk measures for electricity markets modelling can be found in [49,57,58]

3. DG units selection, sizing and allocation

This section presents the general formulation of the MOO problem considered previously. As introduced, the practical aim of the MOO is to find the optimal integration of DG in terms of selection, sizing and allocation of the different renewable generation units (including EV and ST). The corresponding decision variables are contained in Ξ^{DG} of the configuration matrix Ξ.

The MOO problem consists in the concurrent minimization of the two objective functions measuring the C_g and *ENS*, and their associated risk. Specifically, their expected values and their *CVaR* values are combined, weighted by a factor $\beta \in [0,1]$, which allows modulating the expected performance of the distribution network and its associated risk.

3.1. MOO problem formulation

Considering a set of randomly generated scenarios Υ, the optimization problem is formulated as follows:

$$\min \quad f_1 = \beta EC_g^{\Upsilon} + (1-\beta) CVaR_\alpha(C_g^{\Upsilon}) \tag{40}$$

$$\min \quad f_2 = \beta EENS^{\Upsilon} + (1-\beta) CVaR_\alpha(ENS^{\Upsilon}) \tag{41}$$

s.t.

$$\xi_{i,j} = \begin{cases} \zeta & \text{number of units of the MS type or DG technology } j \text{ allocated at node } i \\ 0 & \text{otherwise} \end{cases}$$
$$\forall i \in N, j \in MS \cup DG, \zeta \in Z^* \tag{2}$$

$$\sum_{i \in N} \sum_{j \in DG} \xi_{i,j} (C_{inv_j} + C_{O\&M_j}) \le BGT \tag{42}$$

$$\sum_{i \in N} \xi_{i,j} \le \tau_j \quad \forall j \in DG \tag{43}$$

$$\text{OPF}(\{\Xi, FD\}, \Upsilon) \tag{28)–(33}$$

where EC_g and *EENS* denote the expected values of C_g and *ENS*, respectively.

The meaning of each constraint is, (2)—the decision variable $\xi_{i,j}$ is a non-negative integer number; (42)—the total costs of investment and fixed operation and maintenance of the DG units must be less or equal to the available budget *BGT*; (43)—the total number of DG units to allocate of each technology j must be less or equal to the maximum number of units available τ_j to be

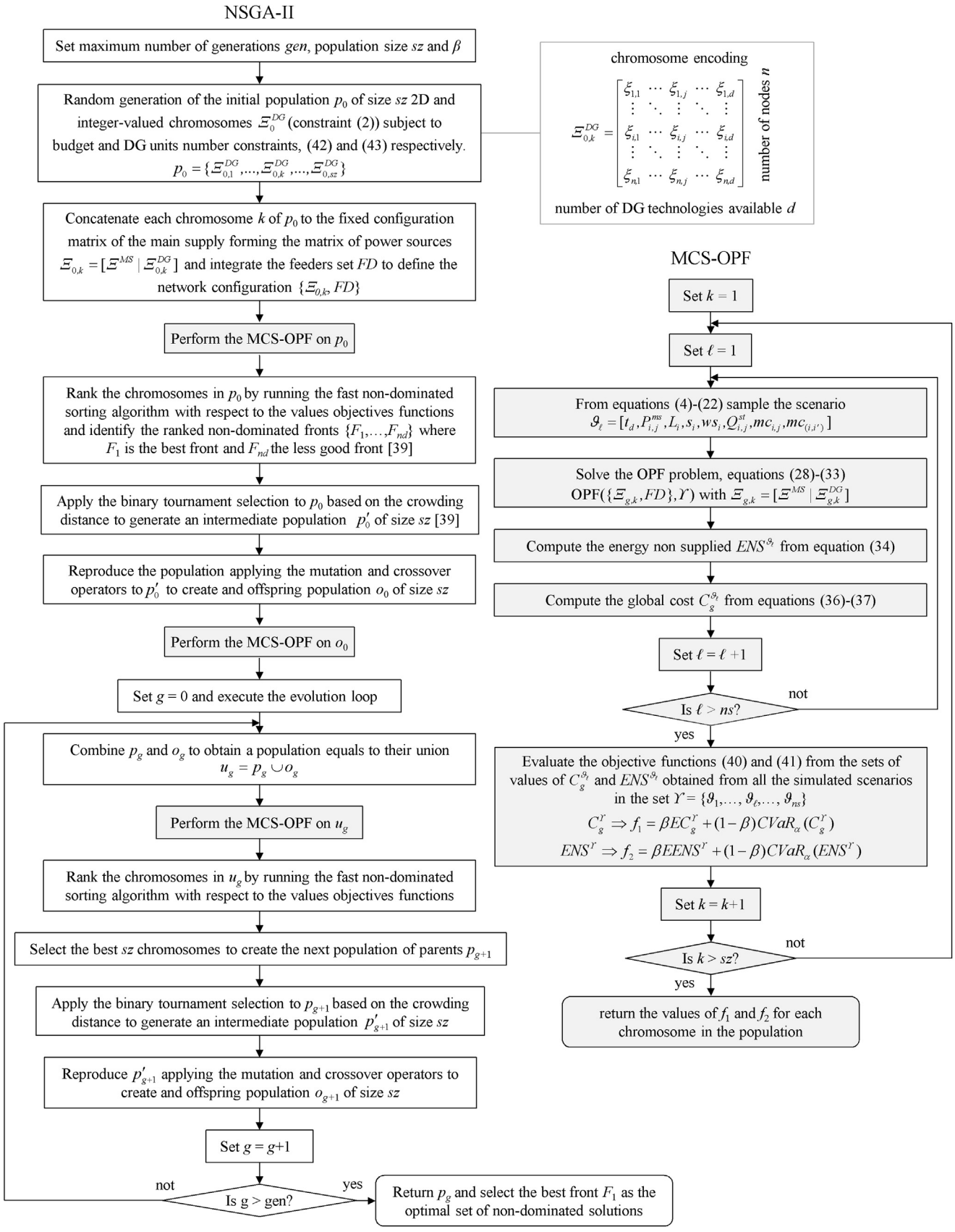

Fig. 7. Flow chart of NSGA-II MCS-OPF MOO framework.

integrated; (28)–(33)—all the equations of OPF must be satisfied for all scenarios in Υ.

Constraint (43) can be translated into maximum allowed penetration factor $PF^{DG}_{\max_j}$ of each DG technology j. Defining PF as 'the output active power of total capacity of DG divided by the total network load' [59], constraint (43) can be rewritten as follows:

$$\underbrace{\frac{\sum_{i\in N}\xi_{i,j}EP_j^{DG}}{EL_T}}_{PF_j^{DG}} \le \underbrace{\frac{\tau_j EP_j^{DG}}{EL_T}}_{PF^{DG}_{\max_j}} \quad \forall j \in DG \tag{44}$$

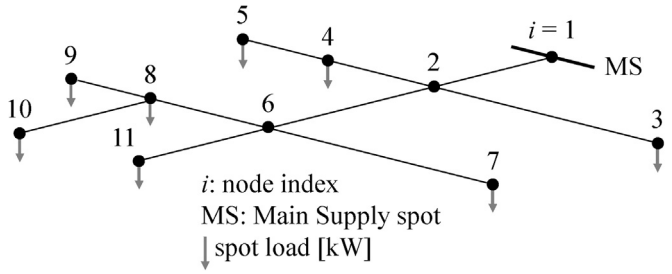

Fig. 8. Radial 11-nodes distribution network.

Table 1
Feeders characteristic and technical data [40].

Type	Node i	Node i'	Length [km]	X [Ω/km]	Amp [A]
T1	1	2	0.61	0.37	365
T2	2	3	0.15	0.47	170
T3	2	4	0.15	0.56	115
T1	2	6	0.61	0.37	*365*
T3	4	5	0.09	0.56	115
T6	6	7	0.15	0.25	165
T4	6	8	0.09	0.56	115
T1	6	11	0.31	0.37	365
T5	8	9	0.09	0.56	115
T7	8	10	0.24	0.32	115

Table 2
Main power supply parameters.

Node i	P^{ms}_{cap} [kW]	Normal distribution parameters	
		μ^{ms}	σ^{ms}
1	1600	1200	27.5

where $\sum_{i\in N}\xi_{i,j}$—is the total number of units of DG technology j integrated in the network; EP_j^{DG}—is the expected power output of one unit of DG technology j [kW]; EL_T—is the expected total load [kW].

The MOO optimization problem is non-linear and non-convex, i.e., a non-convex mixed-integer non-linear problem or non-convex MINLP. It is non-linear because the objective functions given by Eqs. (40) and (41) cannot be written in the canonical form of a linear program, i.e., C^TX, where C a vector of known coefficients and X the decision vector. In the present case, the decision matrix Ξ^{DG} enters the MCS-OPF flow simulation to obtain the probability mass functions of C_g and ENS and, then, the objective functions are formed from the corresponding expected and $CVaR$ values. Thus, the operations applied on Ξ^{DG} through MCS-OPF, expectation and $CVaR$ cannot not be represented as the product $C^T\Xi^{DG}$. The problem is non-convex because the decision matrices Ξ^{DG} are integer-valued (constraint (2)) and, as it is known, the set of non-negative integers is non-convex.

Given the class of optimization problems in the proposed framework (non-convex MINLP), it is most likely to have multiple local minima. Moreover, the dimension of the distribution network can lead to a combinatorial explosion of the feasible space of the decision matrices Ξ^{DG} [7,10], incrementing the number of possible local minima and hindering the possibility of benchmarking the optimal solutions obtained. However, an approximated but straightforward alternative is to perform several realizations of the framework obtaining different optimal solutions under the same optimization and simulation conditions (parameters) and, thus, compare them regarding the optimal decision matrices and their associated value of the objective functions.

Table 3
Parameters of PV, W, EV and ST technologies [11,13,42].

PV		W	
Beta distribution α	0.26	Rayleigh distribution σ	7.96
Beta distribution β	0.73	P^{w}_{RTD} [kW]	50
T_a [°C]	30	ws_{ci} [m/s]	3.8
N_{oT} [°C]	43	ws_a [m/s]	9.5
I_{sc} [A]	1.8	ws_{co} [m/s]	*23.8*
k_i [mA/°C]	1.4	EV	
V_{oc} [V]	55.5	P^{ev}_{RTD} [kW]	6.3
k_v [mV/°C]	194	ST	
V_{MPP} [V]	38	P^{st}_{RTD} [kW]	0.275
I_{MPP} [A]	1.32	SE [kJ/kg]	0.042

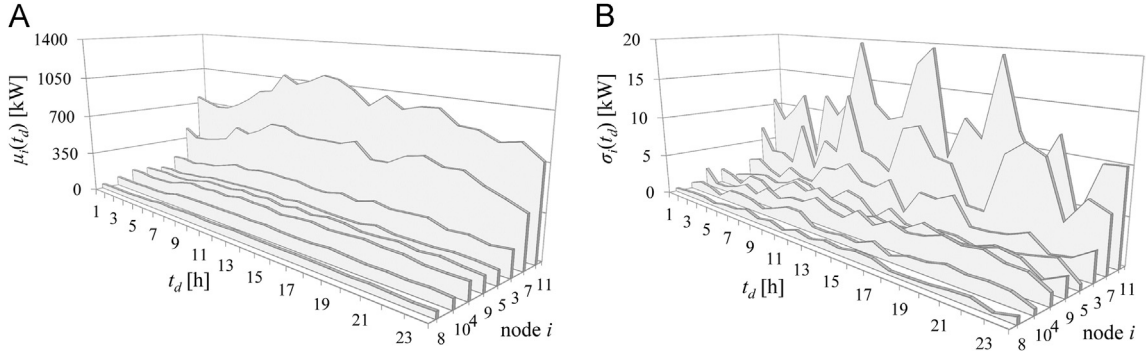

Fig. 9. Mean (A) and variance (B) values of nodal power demand daily profiles.

This process was performed for the proposed case study. Indeed, the optimal decision matrices Ξ^{DG} are different in all the cases, when the optimization and simulation framework is performed under the same conditions but, nonetheless, practically the same Pareto optimal values of EC_g and *EENS* are eventually obtained. This reflects that equally expected performances (EC_g, *EENS*) can be obtained for different Ξ^{DG} considering the large amount of feasible combinations, which is what is of interest for practical applications.

3.2. NSGA-II with nested MCS-OPF

The combinatorial MOO problem under uncertainties is solved by the NSGA-II algorithm [39], in which the evaluation of the objective functions is performed by the developed MCS-OPF. The NSGA-II is one of the most efficient evolutionary algorithms to solve MOO problems [60]. The extension to MOO entails the integration of Pareto optimality concepts. In general terms, solving a MOO problem of the form:

$$\min \{f_1(X), f_2(X), \ldots, f_k(X)\} \quad \text{subject to } X \in \Lambda \tag{45}$$

with at least two conflicting objectives functions (f_i: $\Re^n \rightarrow \Re$) implies to find, within a set of acceptable solutions that belong to the non-empty feasible region $\Lambda \subset \Re^n$, the decision vectors $X \in \Lambda$ that satisfy the following [61]:

$$\neg\exists X \in \Lambda / f_i(X) \leq f_i(X') \ \forall i = 1, \ldots, k \quad \text{and} \quad f_i(X) < f_i(X') \text{ for at least one } i$$
$$\Downarrow$$
$$f(X) \prec f(X') \text{ i.e. } f(X) \text{ dominates } f(X') \tag{46}$$

X is called a Pareto optimal solution and the Pareto front *PF* is defined as $\{f(X) \in \Re / X \text{ is Pareto optimal solution}\}$.

The process of searching the non-dominated solutions set *PF*, carried out by the NSGA-II MCS-OPF, can be summarized as shown in Fig. 7.

The interested reader can consult [62–64] to compare the proposed framework to alternative MOO analytical approaches in energy applications.

4. Case study

We consider a distribution network adapted from the *IEEE 13 nodes test feeder* [40,65]. The spatial structure of the network has not been altered but we neglect the regulator, capacitor and switch, and remove the feeders of zero length. The network is chosen purposely small, but with all relevant characteristics for the analysis, e.g., comparatively low and high spot and distributed load values and the presence of a power supply spot [65]. The original *IEEE 13 nodes test feeder* is dimensioned such that the total power demand is satisfied without lines overloading. We modify it so that it becomes of interest to consider the integration of renewable DG units. Specifically, the location and values of some of the load spots and the ampacity values of some feeders have been modified in order to generate conditions of power congestion of the lines, leading to shortages of power supply to specific portions of the network.

4.1. Distribution network description

The distribution network presents a radial structure of $n=11$ nodes and $fd=(n-1)=10$ feeders, as shown in Fig. 8. The nominal voltage is $V=4.16$ [kV], constant for the resolution of the DC optimal power flow problem.

Table 1 contains the technical characteristics of the different types of feeders considered: specifically, the indexes of the pairs of nodes that are connected by each feeder of the network, their length, reactance X and their ampacity *Amp*.

Concerning the main power supply spot, the maximum active power capacity of the transformer and the parameters of the normal distribution that describe its variability are given in Table 2.

The nodal power demands are reported as daily profiles, normally distributed on each hour. The mean μ and variance σ values of the nodal daily profiles of the power demands are shown in Fig. 9(A) and (B), respectively.

The technical parameters of the four different types of DG technologies available to be integrated into the distribution network (PV, W, EV and ST) are given in Table 3. The values of the parameters of the Beta and Rayleigh distributions describing the variability of the solar irradiation and wind speed, are assumed constant in the whole network, i.e., the region of distribution is such that the weather conditions are the same for all nodes.

The hourly per day operating states probability profile of the EV is presented in Fig. 10 and failures and repair rates of the components of the distribution network are provided in Table 4.

The values of the investment (C_{inv}) and fixed and variable Operational and Maintenance ($C_{O\&M^f}$ and $C_{O\&M^v}$) costs of the MS and DG units are reported in Table 5. Consistently with the constraints (42) and (43) of the MOO problem, the total investment associated to a decision variable Ξ^{DG} (proposed by the NSGA-II) must be less than or equal to the limit budget; which is set to $BGT=4500000$ [$], and the total number of units of each type of DG (following the order [*PV*, *W*, *EV*, *ST*]) must be less than

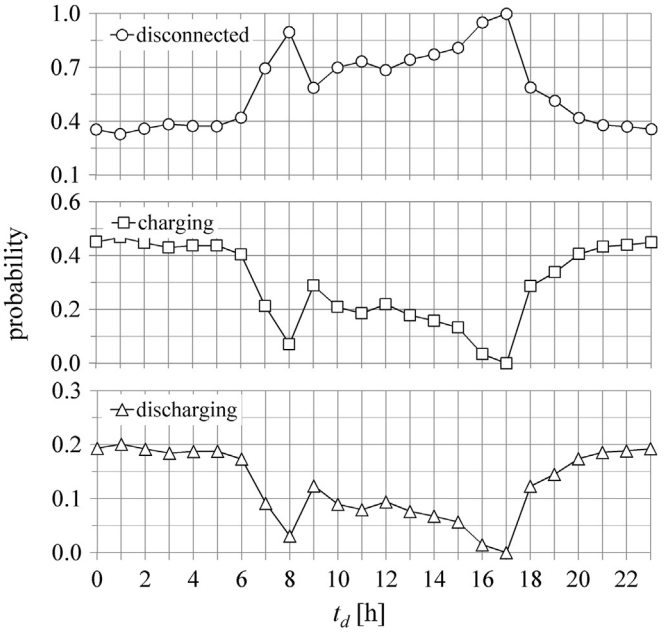

Fig. 10. Hourly per day probability data of EV operating states.

Table 4
Failure rates of feeders, MS and DG units [11,13,42,66].

Type		λ^F [failures/h]		λ^R [repairs/h]	
MS∪DG	*FD*	*MS∪DG*	*FD*	*MS∪DG*	*FD*
MS	*T1*	3.33E−04	3.33E−04	0.021	0.198
PV	*T2*	4.05E−04	4.05E−04	0.013	0.162
W	*T3*	3.55E−04	3.55E−04	0.015	0.185
EV	*T4*	3.55E−04	3.55E−04	0.105	0.185
ST	*T5*	3.55E−04	3.55E−04	0.073	0.185
–	*T6*	–	4.00E−04	–	0.164
–	*T7*	–	3.55E−04		

or equal to τ=[15000, 5, 200, 8000]. The value of the incentive for renewable kW h supplied is taken as 0.024 [$/kW h] [34]. The maximum value of the energy price ep_h is 0.11 [$/kW h] [19,20]. Concerning the calculation of the *CVaR*, the alpha-percentile is taken as α=0.80.

Five optimizations runs of the NSGA-II with the nested MCS-PF algorithm have been performed, each one with a different value of the weight parameter $\beta \in \{1, 0.75, 0.5, 0.25, 0\}$, to analyze different tradeoffs between optimal average performance and risk. From Eqs. (40) and (41), note that the value β=1 corresponds to optimizing only the expected values of *ENS* and C_g, whereas β=0 corresponds to the opposite extreme case of optimizing only the *CVaR* values. Each NSGA-II run is set to perform g=300 generations over a population of sz=100 chromosomes and, for the reproduction, the single-point crossover and mutation genetic operators are used. The crossover probability is pco=1, whereas the mutation probability is pmu=0.1; the mutation can occur simultaneously in any bit of the chromosome.

Finally, sn=250 random scenarios are simulated by the MCS-OPF with time step t^s=1 [h]. Over an horizon of analysis of 10 years (t^h=87600 [h]), in which the investment and fixed costs are prorated hourly.

Table 5
Investment, fixed O&M and variable O&M costs of MS and DG [27,34,66].

Type	$C_{inv}+C_{O\&M^f}$ [$]	$C_{O\&M^v}$ [kW h]
MS	–	1.45E−01
PV	48	3.76E−05
W	113750	3.90E−02
EV	17000	2.20E−02
ST	135.15	4.62E−05

4.2. Results and discussion

The Pareto fronts resulting from the NSGA-II MCS-OPF are presented in Fig. 11 for the different values of β. The 'last generation' population is shown and the non-dominated solutions are marked in bold.

Each non-dominated solution in the different Pareto fronts corresponds to an optimal decision matrix Ξ^{DG} for the sizing and allocation of DG, i.e., an optimal DG-integrated network configuration $\{\Xi, FD\}$ where $\Xi=[\Xi^{MS}|\Xi^{DG}]$.

In the Pareto fronts obtained, we look of three representative non-dominated solutions for the analysis: those with minimum values of the objective functions f_1 and f_2 independently ($\Xi^{DG}_{\min f_1}$ and $\Xi^{DG}_{\min f_2}$, respectively) and an intermediate solution at the 'elbow' of the Pareto front. Table 6 presents the values of the objective functions, *EENS*, EC_g and their respective *CVaR* values for the selected solutions. The *EENS*, EC_g and *CVaR* values of the case in which no DG is integrated in the network (MS case) is also reported.

Fig. 12 shows a bubble plot representation of the selected optimal solutions. The axes report the *EENS* and EC_g values while the diameters of the bubbles are proportional to their respective *CVaR* values. The MS case is also plotted.

From Table 6 and Fig. 12 it can be seen that, the MS case has an expected performance (*EENS*=1109.21 [kW h] and EC_g=170.27 [$]) inferior (high *EENS* and EC_g) to any case for which DG is optimally integrated. Furthermore, the *CVaR*(*ENS*)=1656.53 [kW h] for the MS case is the highest, indicating the high risk of actually achieving the expected performance of energy not supplied. This confirms that DG is capable of providing a gain of reliability of power supply and economic benefits, the risk of falling in scenarios of large amounts of energy not supplied being reduced.

Comparing among the selected optimal DG-integrated networks, in general the expected performances of *EENS* and EC_g are progressively

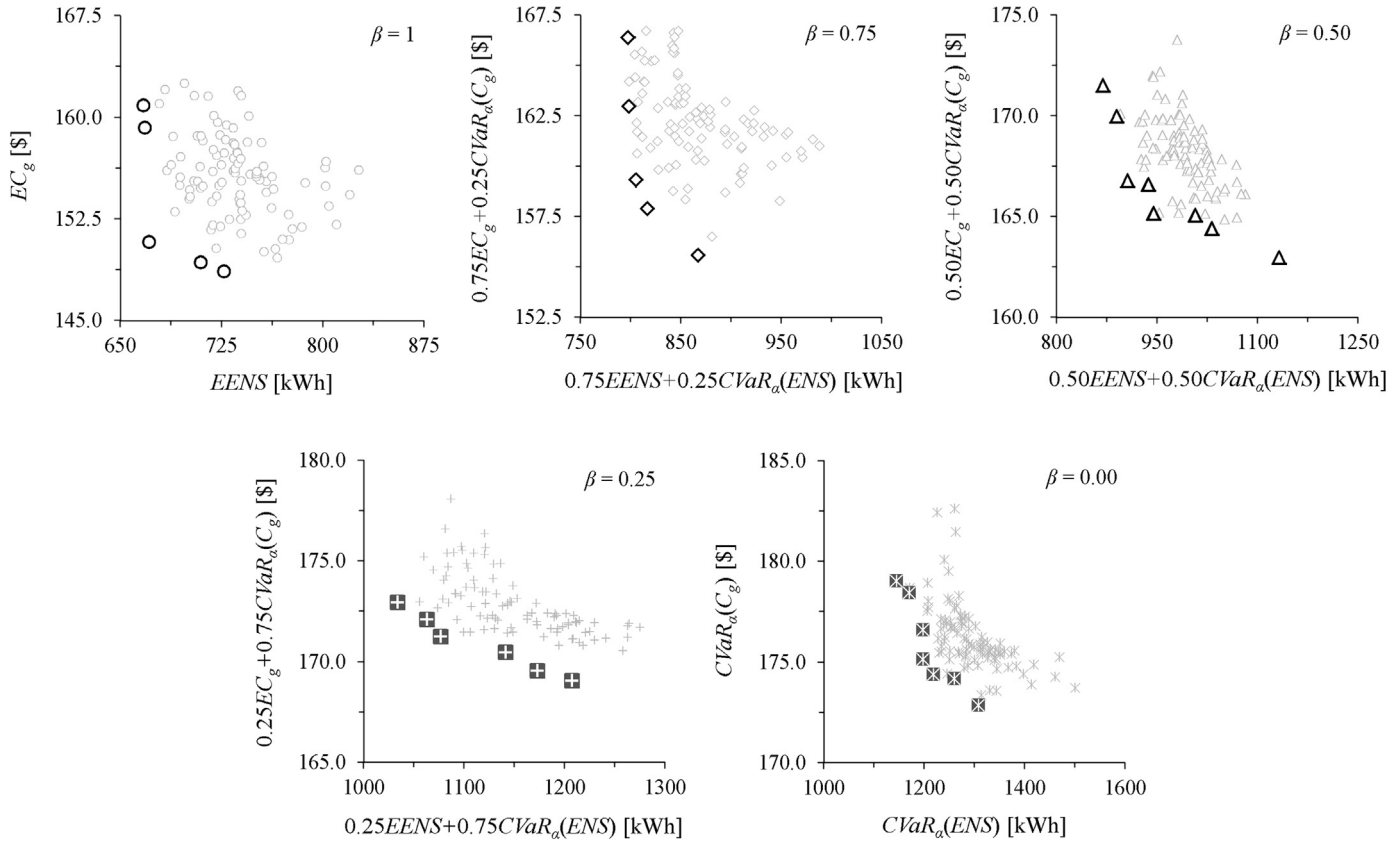

Fig. 11. Pareto fronts for different values of β.

Table 6
Objective functions: expected and *CVaR* values of selected Pareto front solutions.

	β	f_1 [kW h]	f_2 [kW h]	*EENS* [kW h]	*CVaR*(*ENS*) [kW h]	EC_g [$]	*CVaR*(C_g) [$]
MS	–	–	–	1109.21	1656.53	170.27	179.24
$\Xi^{DG}_{\min f_1}$	1.00	666.95	160.91	666.95	1093.12	160.91	185.11
Ξ^{DG}_{elbow}		671.05	150.83	671.05	1185.53	150.83	179.47
$\Xi^{DG}_{\min f_2}$		726.57	148.68	726.57	1279.37	148.68	178.23
$\Xi^{DG}_{\min f_1}$	0.75	797.07	166.41	677.74	1155.11	160.68	183.62
Ξ^{DG}_{elbow}		805.27	159.35	697.17	1129.62	153.09	178.15
$\Xi^{DG}_{\min f_2}$		867.08	155.61	729.81	1278.94	147.66	179.45
$\Xi^{DG}_{\min f_1}$	0.50	868.61	171.54	641.68	1095.52	159.43	183.64
Ξ^{DG}_{elbow}		936.58	166.67	701.72	1171.47	154.67	178.53
$\Xi^{DG}_{\min f_2}$		1131.64	162.99	843.53	1419.79	150.45	175.58
$\Xi^{DG}_{\min f_1}$	0.25	1033.65	172.95	723.19	1137.18	156.55	178.42
Ξ^{DG}_{elbow}		1076.53	171.25	743.61	1187.43	156.32	176.24
$\Xi^{DG}_{\min f_2}$		1207.33	169.07	835.23	1331.34	158.64	173.47
$\Xi^{DG}_{\min f_1}$	0.00	1144.36	179.03	744.71	1144.31	163.82	179.03
Ξ^{DG}_{elbow}		1197.79	176.62	749.21	1197.74	160.93	176.62
$\Xi^{DG}_{\min f_2}$		1307.33	172.87	828.55	1307.35	159.78	172.87

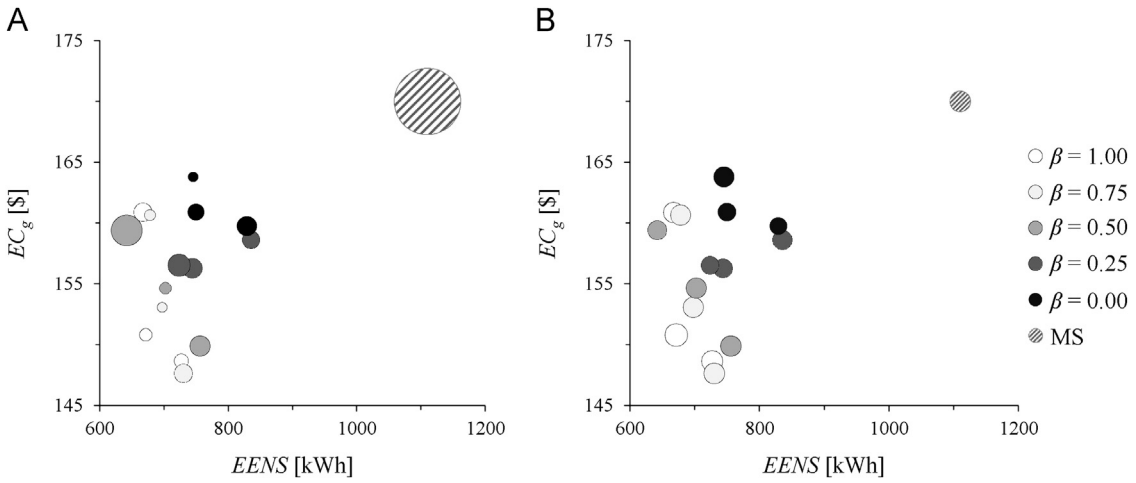

Fig. 12. Bubble plots *EENS* v/s EC_g. Diameter of bubbles proportional to *CVaR*(*ENS*) (A) and *CVaR*(C_g) (B).

lower for increasing β. This to be expected: lowering the values of β, the MOO tends to search for optimal allocations and sizing Ξ^{DG} that sacrifice expected performance at the benefit of decreasing the level of risk (*CVaR*). These insights can serve the decision making process on the integration of renewable DG into the network, looking not only at the give-and-take between the values of *EENS* and, but also at the level of risk of not achieving such expected performances due to the high variability.

Fig. 13 shows the average total DG power allocated in the distribution network and its breakdown by type of DG technology for the optimal Ξ^{DG} as a function of β. It can be pointed out that the contribution of EV is practically negligible if compared with the other technologies. This is due to the fact that the probability that the EV is in a discharging state is much lower than that of being in the other two possible operating states, charging and disconnected (see Fig. 10), combined with the fact that when EV is charging the effects are opposite to those desired.

The analysis of the results for different β values also allows highlighting the impact that each type of renewable DG technology has on the network performance. As can be noticed in Fig. 13(A), the average total renewable DG power optimally allocated, increases progressively for increasing values of β: this could mean that to obtain less 'risky' expected performances less renewable DG power needs to be installed. However, focusing on the individual fractions of average power allocated by PV, W and ST (Fig. 13(B), (C) and (E), respectively), show that a reduction of the risk in the *EENS* and EC_g is achieved specifically diminishing the proportion of PV power (from $0.29_{\beta=1}$ to $0.11_{\beta=0}$) while increasing the W and ST (from $0.38_{\beta=1}$ to $0.48_{\beta=0}$ and from $0.31_{\beta=1}$ to $0.39_{\beta=0}$, respectively), but this increment of W and ST power is not enough to balance the loss of PV power due to the limits imposed by the constraints in the number of each DG technology to be installed given by τ_j. Thus, PV power supply is shown to most contribute to the achievement of optimal expected performances, but with higher levels of risk. On the other hand, privileging the integration of W and ST power supply provides more balanced optimal solutions in terms of expectations and of achieving these expectations.

Table 7 summarizes the minimum, average and maximum total renewable DG power allocated per node. The tendency is to install more localized sources (mainly nodes 4 and 8) of renewable DG power when the MOO searches only for the optimal expected performances ($\beta=1$) and to have a more uniformly allocation of the power when searches for minimizing merely the *CVaR* ($\beta=0$).

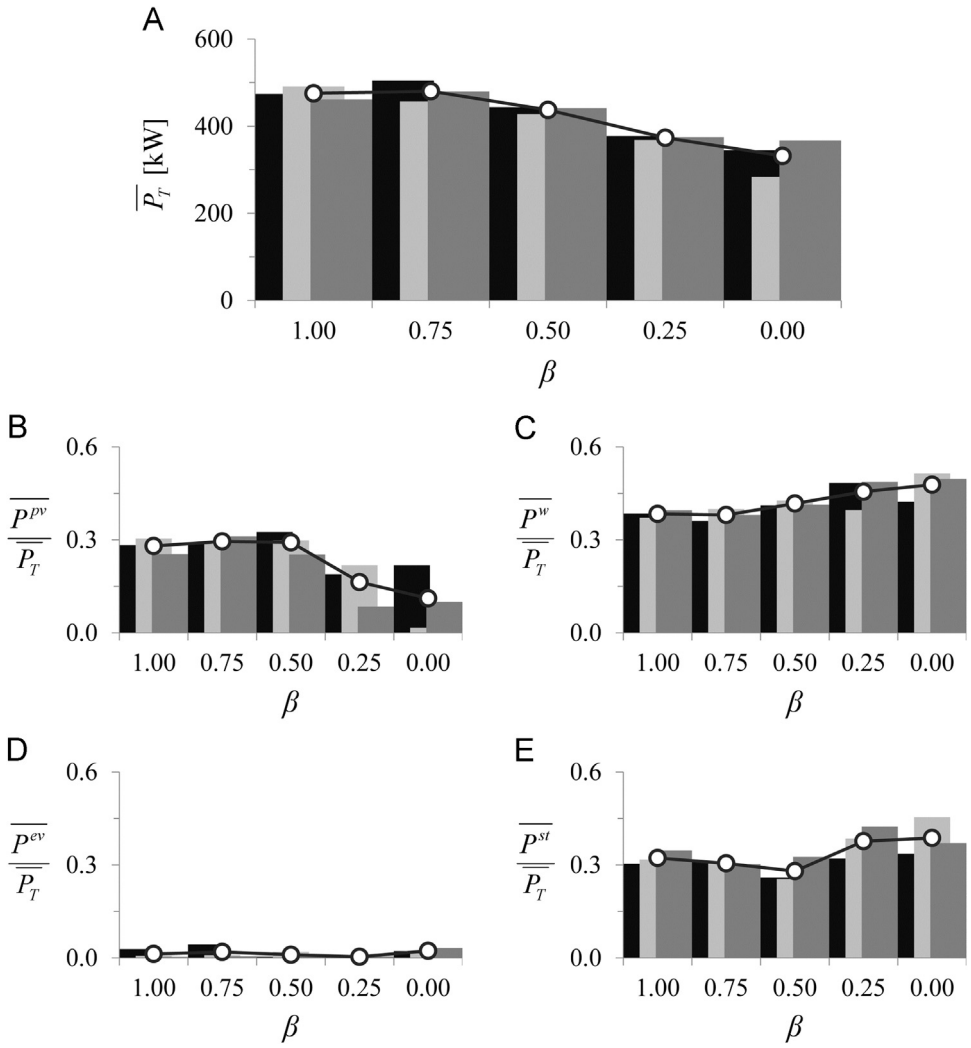

Fig. 13. Average total DG power allocated (A) and its breakdown by type of DG: PV (B), W (C), EV (D) and ST (E).

Table 7
Average, minimum and maximum total DG power allocated per node.

$\overline{P_T}$ [kW]	β														
	1.00			0.75			0.50			0.25			0.00		
Node	Min	Mean	Max	Min	Mean	Max	Min	Mean	Max	Min	Mean	Max	Min	Mean	Max
1	12.08	34.44	54.77	1.15	22.40	38.56	0.00	19.23	40.98	0.00	39.03	121.00	3.00	17.33	34.71
2	2.30	40.72	69.73	0.00	49.95	77.70	36.50	58.40	123.36	3.00	63.61	132.93	0.00	42.54	84.09
3	0.00	24.83	46.45	14.80	41.79	85.03	0.00	37.94	105.11	4.00	36.87	98.53	1.00	32.84	77.78
4	76.00	110.00	133.41	1.15	67.40	133.63	0.58	38.04	80.13	6.15	20.73	61.85	0.00	39.85	85.86
5	22.60	52.39	77.08	28.90	60.66	98.59	12.63	89.39	143.50	3.30	23.49	54.25	1.00	24.97	79.64
6	12.33	55.56	85.46	10.45	21.22	38.95	2.00	27.68	106.26	12.15	53.78	84.43	0.00	50.64	116.85
7	8.00	16.52	35.38	39.38	64.07	104.05	0.00	52.03	159.73	0.00	34.09	92.81	5.00	18.51	39.23
8	79.03	111.20	146.63	30.00	74.57	114.41	0.00	40.60	146.06	4.00	37.94	102.60	1.00	39.49	119.38
9	0.00	20.03	68.73	4.00	74.07	107.88	0.00	46.72	85.61	0.00	44.06	94.08	0.00	32.86	74.53
10	0.00	9.07	25.35	0.00	1.58	7.88	0.00	11.88	58.69	0.00	8.58	43.40	0.00	30.12	83.45
11	0.00	9.98	17.68	0.00	3.04	13.20	0.00	4.74	23.45	0.00	8.99	45.95	0.00	7.31	51.17

5. Conclusions

We have presented a risk-based simulation and multi-objective optimization framework for the integration of renewable generation into a distribution network. The inherent uncertain behavior of renewable energy sources and variability in the loads are taken into account, as well as the possibility of failures of network components. For managing the risk of not achieving expected performances due to the multiple sources of uncertainty, the conditional value-at-risk is introduced in the objective functions, weighed by a β parameter

which allows trading off the level of risk. The proposed framework integrates the Non-dominated Sorting Genetic Algorithm II as a search engine, Monte Carlo simulation to randomly generate realizations of the uncertain operational scenarios and Optimal Power Flow to model the electrical distribution network flows. The optimization is done to simultaneously minimize the energy not supplied and global cost, combined with their respective conditional value-at-risk values in an amount controlled by β.

To exemplify the proposed framework, a case study has been analyzed derived from the *IEEE 13 nodes test* feeder. The results obtained show the capability of the framework to identify Pareto optimal sets of renewable DG units allocations. Integrating the conditional value-at-risk into the framework and performing optimizations for different values of β has shown the possibility of optimizing expected performances while controlling the uncertainty in its achievement. The contribution of each type of renewable DG technology can also be analyzed, indicating which is more suitable for specific preferences of the decision makers.

References

[1] Atwa YM, El-Saadany EF, Salama MMA, Seethapathy R. Optimal renewable resources mix for distribution system energy loss minimization. IEEE Trans Power Syst 2010;25:360–70.

[2] Celli G, Ghiani E, Mocci S, Pilo F. A multiobjective evolutionary algorithm for the sizing and siting of distributed generation. IEEE Trans Power Syst 2005;20:750–7.

[3] Liu Z, Wen F, Ledwich G. Optimal siting and sizing of distributed generators in distribution systems considering uncertainties. IEEE Trans Power Delivery 2011;26:2541–51.

[4] Akorede MF, Hizam H, Pouresmaeil E. Distributed energy resources and benefits to the environment. Renewable Sustainable Energy Rev 2010;14:724–34.

[5] Alanne K, Saari A. Distributed energy generation and sustainable development. Renewable Sustainable Energy Rev 2006;10:539–58.

[6] Karger CR, Hennings W. Sustainability evaluation of decentralized electricity generation. Renewable Sustainable Energy Rev 2009;13:583–93.

[7] Martins VF, Borges CLT. Active distribution network integrated planning incorporating distributed generation and load response uncertainties. IEEE Trans Power Syst 2011;26:2164–72.

[8] Viral R, Khatod DK. Optimal planning of distributed generation systems in distribution system: a review. Renewable Sustainable Energy Rev 2012;16:5146–65.

[9] Koutroumpezis GN, Safigianni AS. Optimum allocation of the maximum possible distributed generation penetration in a distribution network. Electr Power Syst Res 2010;80:1421–7.

[10] Alarcon-Rodriguez A, Ault G, Galloway S. Multi-objective planning of distributed energy resources: a review of the state-of-the-art. Renewable Sustainable Energy Rev 2010;14:1353–66.

[11] Raoofat M. Simultaneous allocation of DGs and remote controllable switches in distribution networks considering multilevel load model. Int J Electr Power Energy Syst 2011;33:1429–36.

[12] Lee S-H, Park J-W. Selection of optimal location and size of multiple distributed generations by using Kalman Filter algorithm. IEEE Trans Power Syst 2009;24:1393–400.

[13] Falaghi H, Singh C, Haghifam M-R, Ramezani M. DG integrated multistage distribution system expansion planning. Int J Electr Power Energy Syst 2011;33:1489–97.

[14] Celli G, Mocci S, Pilo F, Soma GG. A multi-objective approach for the optimal distributed generation allocation with environmental constraints. In: Probabilistic methods applied to power systems, 2008 PMAPS '08 proceedings of the 10th international conference on; 2008. p. 1–8.

[15] Mohammed YS, Mustafa MW, Bashir N, Mokhtar AS. Renewable energy resources for distributed power generation in Nigeria: a review of the potential. Renewable Sustainable Energy Rev 2013;22:257–68.

[16] Borges CLT, Martins V-cF. Multistage expansion planning for active distribution networks under demand and distributed generation uncertainties. Int J Electr Power Energy Syst 2012;36:107–16.

[17] Celli G, Pilo F, Soma GG, Gallanti M, Cicoria R. Active distribution network cost/benefit analysis with multi-objective programming. In: Electricity distribution —Part 1, 2009 CIRED 2009 20th international conference and exhibition on; 2009. p. 1–5.

[18] Hejazi HA, Hejazi MA, Gharehpetian GB, Abedi M. Distributed generation site and size allocation through a techno economical multi-objective differential evolution algorithm. Power and energy (PECon), 2010 IEEE international conference on; 2010. p. 874–849.

[19] Ren H, Gao W. A MILP model for integrated plan and evaluation of distributed energy systems. Appl Energy 2010;87:1001–14.

[20] Ren H, Zhou W, Kat Nakagami, Gao W, Wu Q. Multi-objective optimization for the operation of distributed energy systems considering economic and environmental aspects. Appl Energy 2010;87:3642–51.

[21] El-Khattam W, Bhattacharya K, Hegazy Y, Salama MMA. Optimal investment planning for distributed generation in a competitive electricity market. IEEE Trans Power Syst 2004;19:1674–84.

[22] El-Khattam W, Hegazy YG, Salama MMA. An integrated distributed generation optimization model for distribution system planning. IEEE Trans Power Syst 2005;20:1158–65.

[23] Ganguly S, Sahoo NC, Das D. A novel multi-objective PSO for electrical distribution system planning incorporating distributed generation. Energy Syst 2010;1:291–337.

[24] Gomez-Gonzalez M, LÃ³pez A, Jurado F. Optimization of distributed generation systems using a new discrete PSO and OPF. Electr Power Syst Res 2012;84:174–80.

[25] Harrison GP, Piccolo A, Siano P, Wallace AR. Hybrid GA and OPF evaluation of network capacity for distributed generation connections. Electr Power Syst Res 2008;78:392–8.

[26] Ouyang W, Cheng H, Zhang X, Yao L. Distribution network planning method considering distributed generation for peak cutting. Energy Convers Manage 2010;51:2394–401.

[27] Zou K, Agalgaonkar AP, Muttaqi KM, Perera S. Multi-objective optimisation for distribution system planning with renewable energy resources. In: Energy conference and exhibition (EnergyCon), 2010 IEEE international; 2010. p. 670–675.

[28] Borges CLT. An overview of reliability models and methods for distribution systems with renewable energy distributed generation. Renewable Sustainable Energy Rev 2012;16:4008–15.

[29] Wang L, Singh C. Multicriteria design of hybrid power generation systems based on a modified particle swarm optimization algorithm. IEEE Trans Energy Convers 2009;24:163–72.

[30] Ochoa LF, Harrison GP. Minimizing energy losses: optimal accommodation and smart operation of renewable distributed generation. IEEE Trans Power Syst 2011;26:198–205.

[31] Zhao J, Foster J. Flexible transmission network planning considering distributed generation impacts. IEEE Trans Power Syst 2011;26:1434–43.

[32] Tan W-S, Hassan MY, Majid MS, Abdul Rahman H. Optimal distributed renewable generation planning: a review of different approaches. Renewable Sustainable Energy Rev 2013;18:626–45.

[33] Alarcon-Rodriguez A, Haesen E, Ault G, Driesen J, Belmans R. Multi-objective planning framework for stochastic and controllable distributed energy resources. Renewable Power Gener IET 2009;3:227–38.

[34] Pilo F, Celli G, Mocci S, Soma GG. Active distribution network evolution in different regulatory environments. In: Power generation, transmission, distribution and energy conversion (MedPower 2010), seventh Mediterranean conference and exhibition on; 2010. p. 1–8.

[35] Soroudi A, Ehsan M. A possibilistic, Âîprobabilistic tool for evaluating the impact of stochastic renewable and controllable power generation on energy losses in distribution networks, ÃîA case study. Renewable Sustainable Energy Rev 2011;15:794–800.

[36] Hejazi HA, Araghi AR, Vahidi B, Hosseinian SH, Abedi M, Mohsenian-Rad H. Independent distributed generation planning to profit both utility and DG investors. IEEE Trans Power Syst 2013;28:1170–8.

[37] Melnikov A, Smirnov I. Dynamic hedging of conditional value-at-risk. Insuran: Math Econ 2012;51:182–90.

[38] Rockafellar RT, Uryasev S. Conditional value-at-risk for general loss distributions. J Bank Finance 2002;26:1443–71.

[39] Deb K, Pratap A, Agarwal S, Meyarivan T. A fast and elitist multiobjective genetic algorithm: NSGA-II. IEEE Trans Evol Comput 2002;6:182–97.

[40] IEEE power and energy society. Distribution test feeders.

[41] Li Y, Zio E. Uncertainty analysis of the adequacy assessment model of a distributed generation system. Renewable Energy 2012;41:235–44.

[42] Li Y-F, Zio E. A multi-state model for the reliability assessment of a distributed generation system via universal generating function. Reliab Eng Syst Saf 2012;106:28–36.

[43] Clement-Nyns K, Haesen E, Driesen J. The impact of vehicle-to-grid on the distribution grid. Electr Power Syst Res 2011;81:185–92.

[44] Diaz-Gonzalez F, Sumper A, Gomis-Bellmunt O, Villafafila-Robles R. A review of energy storage technologies for wind power applications. Renewable Sustainable Energy Rev 2012;16:2154–71.

[45] Thornton A, Monroy CRg. Distributed power generation in the United States. Renewable Sustainable Energy Rev 2011;15:4809–17.

[46] Zio E. The Monte Carlo simulation method for system reliability and risk analysis. London: Springer; 2013.

[47] Hegazy Y. Adequacy assessment of distributed generation systems using Monte Carlo simulation. IEEE Trans Power Syst 2003;18:48–52.

[48] Shaaban MF, Atwa YM, El-Saadany EF. DG allocation for benefit maximization in distribution networks. IEEE Trans Power Syst 2013;28:639–49.

[49] Samper ME, Vargas A. Investment decisions in distribution networks under uncertainty with distributed generation-Part II: Implementation and results. IEEE Trans Power Syst 2013;28:2341–51.

[50] Purchala K, Meeus L. Usefulness of DC power flow for active power flow analysis. Power Eng Optimiz 2005.

[51] Hertem DV. Usefulness of DC power flow for active power flow analysis with flow controlling devices. AC and DC power transmission. IEEE Int Conf 2006.

[52] Billinton R, Allan R. Reliability evaluation of power systems. 2nd Ed.Springer; 1996.

[53] Haffner S, Pereira LFA, Pereira LA, Barreto LS. Multistage model for distribution expansion planning with distributed generation—Part I: Problem formulation. IEEE Trans Power Delivery 2008;23:915–23.
[54] Haffner S, Pereira LFA, Pereira LA, Barreto LS. Multistage model for distribution expansion planning with distributed generation—Part II: Numerical results. IEEE Trans Power Delivery 2008;23:924–9.
[55] Wang LF, Singh C. Multicriteria design of hybrid power generation systems based on a modified particle swarm optimization algorithm. IEEE Trans Energy Convers 2009;24:163–72.
[56] Uryasev S. VaR vs CVaR in risk management and optimization. CARISMA conference; 2010 (presentation).
[57] Ahmadi A, Charwand M, Aghaei J. Risk-constrained optimal strategy for retailer forward contract portfolio. Int J Electr Power Energy Syst 2013;53:704–13.
[58] Gitizadeh M, Kaji M, Aghaei J. Risk based multiobjective generation expansion planning considering renewable energy sources. Energy 2013;50:74–82.
[59] Ugranli F, Karatepe E. Multiple-distributed generation planning under load uncertainty and different penetration levels. Int J Electr Power Energy Syst 2013;46:132–44.
[60] Ak R, Li Y, Vitelli V, Zio E, López Droguett E, Magno Couto Jacinto C. NSGA-II-trained neural network approach to the estimation of prediction intervals of scale deposition rate in oil & gas equipment. Expert Syst Appl 2013;40:1205–12.
[61] Branke J. Multiobjective optimization: interactive and evolutionary approaches. Berlin; New York: Springer; 2008.
[62] Aghaei J, Amjady N. A scenario-based multiobjective operation of electricity markets enhancing transient stability. Int J Electr Power Energy Syst 2012;35:112–22.
[63] Aghaei J, Amjady N, Shayanfar HA. Multi-objective electricity market clearing considering dynamic security by lexicographic optimization and augmented epsilon constraint method. Appl Soft Comput 2011;11:3846–58.
[64] Aghaei J, Akbari MA, Roosta A, Baharvandi A. Multiobjective generation expansion planning considering power system adequacy. Electr Power Syst Res 2013;102:8–19.
[65] Kersting WH. Radial distribution test feeders. IEEE Trans Power Syst 1991;6:975–85.
[66] Webster R. Can the electricity distribution network cope with an influx of electric vehicles? J Power Sources 1999:217–25.